Self-Assembly of Densely Packed ZnO Nanorods Grown Chemically on Porous Silicon Substrate

Shabannia, Reza*+; Ghasemtabar, Mahdi

Department of Physics, College of Science, Noshirvani Babol University of Technology, 484, Babol, I.R. IRAN

ABSTRACT: *Self-assembly of densely packed ZnO nanorods were grown on Porous Silicon (PS) substrate by low-temperature chemical bath deposition. The structural and optical properties of the obtained ZnO nanostructures on PS substrate were systematically studied. The strong and sharp (002) peak compared with other peaks in the X-Ray Diffraction (XRD) indicated that ZnO nanorods formed with superior orientation toward the (002) plan. In addition, the small crystallite size and low compressive strain revealed that the self-assembly of densely packed ZnO nanorods had good crystallinity. Field-Emission Scanning Electron Microscopy (FESEM) indicated that the self-assembly of densely packed ZnO nanorods occurred on the surface, inside the pores and on the pore walls of the PS substrate. FESEM images indicated that the average diameter and length of the ZnO nanorods were 150 and 500 nm, respectively. Photoluminescence spectra (PL) exhibited a strong, sharp UV emission peak at 369 nm.*

KEY WORDS: *ZnO nanorods; Porous materials; Crystal structure; Chemical bath deposition.*

INTRODUCTION

ZnO nanostructure with a direct wide band gap of 3.37 eV and large exciton binding energy of 60 meV are widely used because of their potential applications for the development of novel optoelectronic and electronic devices. Such devices include light-emitting diodes, transparent conducting oxides, electron acceptors in hybrid solar cells, photocatalysis, and piezoelectronics [1-10]. Porous semiconductors were extensively investigated in past decades because of their optical properties such as improved photoresponse, band–gap shift, and enhanced luminescence intensity [11]. Porous Silicon (PS) is intensively studied among porous semiconductors because PS substrate has a large internal surface, strong absorbability, high resistance, and potential for the development of silicon-based optoelectronic devices [12]. PS substrates can reduce large mismatches in lattice constants, and thermal expansion coefficients result in high stress between ZnO nanostructures and Si substrates [13]. Abdulgafour et al. [14] fabricated a ZnO nanocoral reef on PS substrates without any catalyst via the simple thermal evaporation method. *Hsu et al.* [12] reported the enhancement of ZnO nanowire orientation on PS using a vapor–liquid–solid method. However, these methods are high-temperature processes that use expensive apparatuses and complicated procedures. Hence, the Chemical Bath Deposition (CBD) method [16] is an appropriate technique for the growth of ZnO nanostructures because it is a simple, low-temperature, low-cost, and scalable process. In this study, we characterized the optical and structural properties of ZnO nanostructures grown by CBD method on seed-layer ZnO/PS substrate.

EXPERIMENTAL SECTION

The experimental setup and synthesis method were as described in our previous study [17]. In a typical procedure, PS substrates were formed on n-type Si (100) wafer by photo-electrochemical etching in a Teflon cell containing a mixture of hydrofluoric acid and ethanol (96%) at a 1:4 volume ratio. PS substrate formation was carried out at room temperature using Pt wire and Si wafer as cathode and anode, respectively. A current density of 20 mA/cm^2 and etching time of 20 min were applied to produce the PS substrate. A sample was illuminated with a 60 W visible lamp during the etching process. The sample was rinsed in deionized water and was then dried with nitrogen gas after etching. A 70-nm thick ZnO seed layer was deposited on the prepared PS substrate by a Radio Frequency (RF) magnetron sputtering system. The ZnO nanostructures were synthesized on the seed-layer ZnO/PS substrates using CBD method. A 0.050 mol/L amount of zinc nitrate hexahydrate (Zn(NO$_3$)$_2$.6H$_2$O) and an equal molar concentration of hexamethylenetetramine (C$_6$H$_{12}$N$_4$) were separately dissolved in DI water at 80 °C to grow the ZnO nanostructures on the PS substrates. The two solutions were mixed in a beaker, and the samples were vertically dipped inside the beaker. For the fabrication of ZnO nanostructures on the seed layer ZnO/PS substrate, the beaker was placed in an oven at 95 °C for 5 h. The samples were rinsed with DI hot water and were then dried with nitrogen gas.

The crystal structure of the ZnO nanostructures was obtained using X-ray diffraction (PANalytical X'Pert PRO MRD PW3040). The surface morphology of the ZnO nanostructures was characterized by field Emission Scanning Electron Microscopy (FESEM) (model FEI/Nova NanoSEM 450). Photoluminescence (Jobin Yvon HR 800 UV, Edison, NJ, USA) was used to characterize the optical properties of the ZnO nanostructures at room temperature.

RESULTS AND DISCUSSIONS

Fig. 1 shows the X-Ray Diffraction (XRD) patterns of the ZnO nanorods grown by CBD on PS substrate. All XRD peaks matched the wurtzite hexagonal phase of bulk ZnO (ICSD 01-080-0074), except for the peak located at 69° and 49° that was related to the PS layer. The ZnO nanostructures favor growth in the (002)
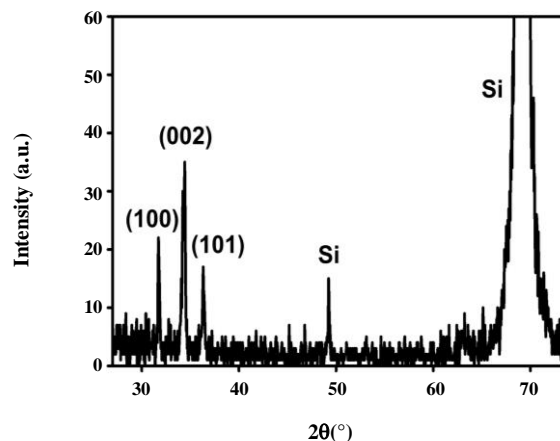

Fig. 1: XRD patterns of the ZnO nanostructures grown on PS substrate.

orientation because the surface free-energy density of the (002) orientation is lowest in a ZnO crystal [18]. In addition, PS is fabricated using a small current density to achieve a silicon surface morphology that exhibits a (111) direction and to assist the growth of ZnO nanorods in the (002) direction [15]. The high intensity of the (002) diffraction peak compared with other peaks in Fig. 1 suggested that the ZnO nanorods formed with superior orientation toward the (002) plan.

The average crystallite size of the ZnO nanostructures along the (002) peak is obtained by the following Scherer equation [19]:

$$D = \frac{0.9\lambda}{\beta \cos\theta} \tag{1}$$

Where *D, θ, λ*, and *β* represent the average crystallite size, Bragg diffraction angle, X-ray radiation wavelength, and full width at half maximum value, respectively. The calculated average crystallite size of the ZnO nanostructures on the PS substrate was determined to be 37 nm. The strain of the ZnO nanostructures synthesized on the PS substrate along the c-axis was obtained by using the following equation [19]:

$$\varepsilon_{zz} = \frac{c - c_0}{c_0} \times 100 \tag{2}$$

Where c and c$_o$ are the lattice constants of the ZnO nanostructures obtained from the XRD data and the standard lattice constant for unstrained ZnO, respectively. The estimated strain was calculated at - 0.002 %;
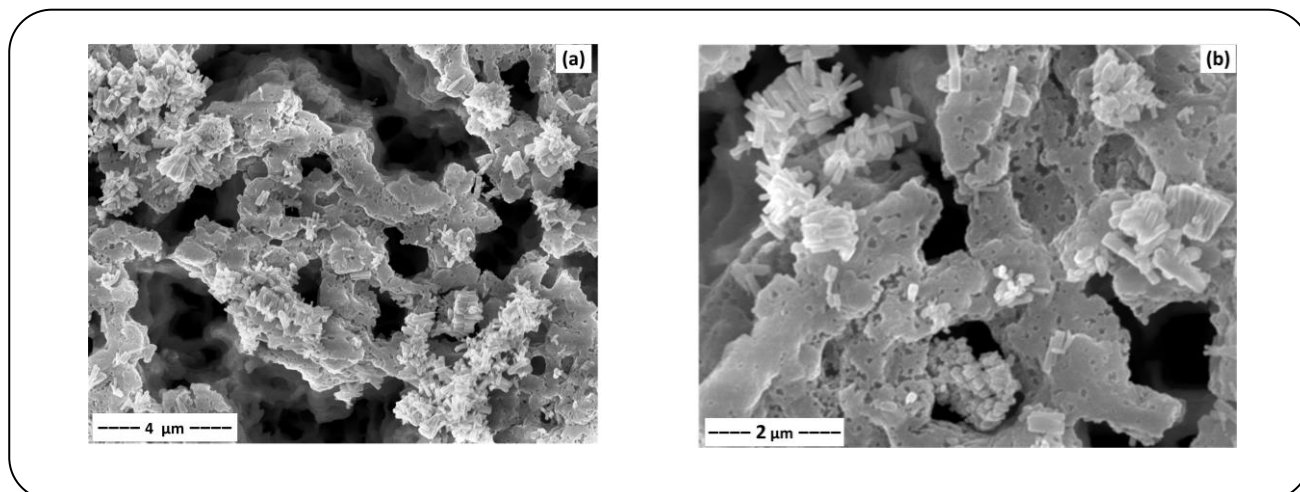
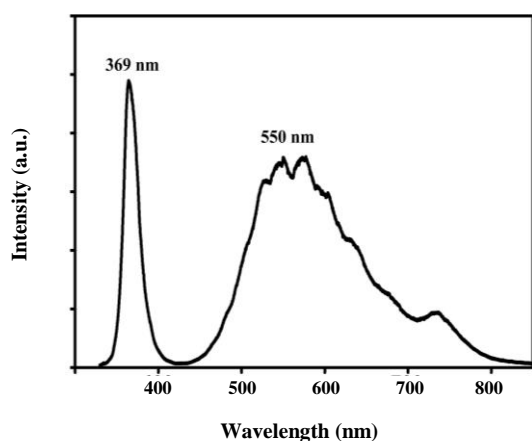*Fig. 2: FESEM image of the ZnO nanostructures grown on PS substrate..*

Fig. 3: PL spectrum of the ZnO nanostructures grown on PS substrate.

a negative value suggests a compressive strain for ZnO nanostructures. In addition, the small crystallite size, low compressive strain, and high intensity at the (002) peak of the ZnO nanostructures grown on PS substrate indicated good crystal quality.

Fig. 2 displays the ZnO nanostructures grown on the PS substrate. Most of obtained ZnO nanostructures were formed from the self-assembly of densely packed ZnO nanorods oriented in different directions. The average diameter and length of the ZnO nanorods were 150 and 500 nm, respectively. Fig. 2(b) clearly shows that the self-assembly of densely packed ZnO nanorods grew on the surface, inside the pores and on the pore walls of the PS substrate. Fig. 2(b) also demonstrates that the self-assembly of densely packed and aligned bilayer

ZnO nanorod arrays occurred inside the pores of PS substrate. Thus, these ZnO nanorods can be used to fabricate gas sensor devices.

The self-assembly of densely packed ZnO nanorods on the seed-layer ZnO/PS substrates were excited using a He-Cd laser with a wavelength of 325 nm at room temperature. Fig. 3 shows the room-temperature photoluminescence spectra of the packed ZnO nanorods synthesized on PS substrate. The presence of sharp and high intensity PL peak at 369 nm is attributed to the near-band-edge UV emission of the ZnO wide band, which originates from the recombination of free excitons through an exciton–exciton collision process [20]. The original UV emission value of the bulk ZnO is 367.655 nm [21]. The redshift in the PL peak of ZnO nanorods towards a longer wavelength at 369 nm are ascribed to Zn vacancies in the ZnO energy band gap. The broad visible emission peak (from 500 nm to 700 nm) was related to the deep-level emission (DLE) of the ZnO band gap, which was due to specific defects, such as oxygen vacancies and zinc interstitials. The presence of small peaks around 740 nm is due to second-order diffraction of high-intensity UV emission (near band edge) peaks [22].

CONCLUSIONS

Self-assembly of densely packed ZnO nanorods were successfully synthesized by CBD on PS substrate. The high intensity and narrow width of the (002) peak ZnO nanostructures grown on PS substrate confirmed that the ZnO nanorods formed with superior orientation toward

the (002) plan. The average crystallite size and compressive strain of the ZnO nanorods were determined to be 37 nm and - 0.002 %, respectively. FESEM image revealed that the self-assembly of the densely packed and aligned bilayer ZnO nanorod arrays occurred inside the pores of PS substrates. The room-temperature PL spectra of these ZnO nanostructures revealed a sharp and high-intensity UV emission peak at 369 nm. Therefore, these self-assembly of the densely packed ZnO nanorods can be used to fabricate UV light detector and gas sensor devices.

REFERENCES

[1] Pouretedal H. R., Basati S., Characterization and Photocatalytic Activity of ZnO, ZnS, ZnO/ZnS, CdO, CdS and CdO/CdS Nanoparticles in Mesoporous SBA-15, *Iran. J. Chem. Chem. Eng. (IJCCE)*, **34:** 11-19 (2015).

[2] Askarinejad A., Alavi M. A., Morsali A., Sonochemically Assisted Synthesis of ZnO Nanoparticles: A Novel Direct, *Iran. J. Chem. Chem. Eng.*, **30:** 75-81 (2011).

[3] Modirshahla N., Behnajady M. A., Jangi Oskui M. R., Investigation of the Efficiency of ZnO Photocatalyst in the Removal of p-Nitrophenol from Contaminated Water, *Iran. J. Chem. Chem. Eng. (IJCCE)*, **28:** 49-55 (2009).

[4] Ghaffarian H. R., Saiedi M., Sayyadnejad M. A., Rashidi A. M., Synthesis of ZnO Nanoparticles by Spray Pyrolysis Method, *Iran. J. Chem. Chem. Eng.*, **30:** 1-6 (2011).

[5] Shabannia R., Hassan H. A., Characteristics of Photoconductive UV Photodetector Based on ZnO Nanorods Grown on Polyethylene Naphthalate Substrate by Chemical Bath Deposition Method, *Electronic Materials Letters*, **10:** 837-43 (2014).

[6] Janitabar Darzi S., Movahedi M., Visible Light Photodegradation of Phenol Using Nanoscale TiO2 and ZnO Impregnated with Merbromin Dye: A Mechanistic Investigation, *Iran. J. Chem. Chem. Eng. (IJCCE)*, **33:** 55-64 (2014).

[7] Jumidali M. M., Sulieman K. M., Hashim M. R., Structural, Optical and Electrical Properties of ZnO/Zn 2 GeO 4 Porous-Like Thin Film and Wires, *Applied Surface Science*, **257:** 4890-5 (2011).

[8] Al-Hardan N., Abdullah M., Aziz A. A., Ahmad H., Low L., ZnO Thin Films for VOC Sensing Applications, *Vacuum* **85:** 101-6 (2010).

[9] Klingshirn C., ZnO: From Basics Ttowards Applications, *Physica Status Solidi (b)*, **244:** 3027-73 (2007).

[10] Arnold M. S., Avouris P., Pan Z. W., Wang Z. L., Field-Effect Transistors Based on Single Semiconducting Oxide Nanobelts, *The Journal of Physical Chemistry B*, **107:** 659-63 (2003).

[11] Chuah L. S., Hassan Z., Ng S. S., Abu Hassan H., Porous Si(111) and Si(100) as An Intermediate Buffer Layer for Nanocrystalline InN Films, *Journal of Alloys and Compounds*, **479:** L54-L8 (2009).

[12] Shaoqiang C., Jian Z., Xiao F., Xiaohua W., laiqiang L., Yanling S., Qingsong X., Chang W., Jianzhong Z., Ziqiang Z., Nanocrystalline ZnO Thin Films on Porous Silicon/Silicon Substrates Obtained by Sol–Gel Technique *Applied Surface Science*, **241:** 384-91 (2005).

[13] Chen J. Y., Sun K. W., Growth of Vertically Aligned ZnO Nanorod Arrays as Antireflection Layer on Silicon Solar Cells, *Solar Energy Materials and Solar Cells*, **94:** 930-4 (2010).

[14] Abdulgafour H. I., F.K.Yam., Hassan Z., Al-Heuseen K., Jawad M. J., ZnO Nanocoral Reef Grown on Porous Silicon Substrates without Catalyst, *Journal of Alloys and Compounds*, **509:** 5627-30 (2011).

[15] Hsu H. C., Cheng C. S., Chang C. C., Yang S., Chang C. S., Hsieh W. F., Orientation-Enhanced Growth and Optical Properties of ZnO Nanowires Grown on Porous Silicon Substrates, *Nanotechnology*, **16:** 297 (2005).

[16] Shabannia R., Vertically Aligned ZnO Nanorods on Porous Silicon Substrates: Effect of Growth time, *Progress in Natural Science: Materials International*, **25:** 95-100 (2015).

[17] Shabannia R., Abu Hassan H., Growth of Aligned ZnO Nanorods Grown on Polyethylene Naphthalate Substrates: Effect of the Growth Duration, *Advanced Materials Research*, **925:** 195-9 (2014).

[18] Lee J., Gao W., Li Z., Hodgson M., Metson J., Gong H., Pal U., Sputtered Deposited Nanocrystalline ZnO Films: A Correlation between Electrical, Optical and Microstructural Properties, *Applied Physics A: Materials Science & Processing*, **80:** 1641-6 (2005).

[19] Shabannia R., Hassan H. A., Controllable Vertically Aligned ZnO Nanorods on Flexible Polyethylene Naphthalate (PEN) Substrate Using Chemical Bath Deposition synthesis, *Applied Physics A,* **114:** 579-84 (2014).

[20] Umar A., Karunagaran B., Suh E., Hahn Y., Structural and Optical Properties of Single-Crystalline ZnO Nanorods Grown on Silicon by Thermal Evaporation, *Nanotechnology*, **17:** 4072 (2006).

[21] Voos M., Uzan P., Delalande C., Bastard G., Halimaoui A., Visible Photoluminescence from Porous Silicon: A Quantum Confinement Effect Mainly Due to Holes?, *Applied Physics Letters*, **61:** 1213-5 (1992).

[22] Tonon C., Duvignacq C., Teyssedre G., Dinguirard M., Degradation of the Optical Properties of ZnO-Based Thermal Control Coatings in Simulated Space Environment, *Journal of Physics D: Applied Physics*, **34:** 124 (2001).